HHS Public Access

Author manuscript

Chembiochem. Author manuscript; available in PMC 2021 May 23.

Published in final edited form as:

Chembiochem. 2019 February 01; 20(3): 360–365. doi:10.1002/cbic.201800651.

Photoinducible Oncometabolite Detection

Rhushikesh A. Kulkarni[a], **Chloe A. Briney**[a], **Daniel R. Crooks**[b], **Sarah E. Bergholtz**[a], **Chandrasekhar Mushti**[c], **Stephen J. Lockett**[d], **Andrew N. Lane**[e], **Teresa W-M. Fan**[e], **Rolf E. Swenson**[c], **W. Marston Linehan**[b], **Jordan L. Meier**[a]

Jordan L. Meier: jordan.meier@nih.gov

[a]Chemical Biology Laboratory, National Cancer Institute, NIH, Frederick MD, 21702, USA

[b]Urologic Oncology Branch, National Cancer Institute, NIH, Bethesda, MD, 20817, USA

[c]Imaging Probe Development Center, National Heart Lung and Blood Institute, National Institutes of Health, Rockville, MD 20850, USA

[d]Optical Microscopy and Analysis Laboratory, Frederick National Laboratory for Cancer Research, Leidos Biomedical Research, Inc., Frederick, MD 21702, USA

[e]Center for Environmental and Systems Biochemistry, Department of Toxicology and Cancer Biology, and Markey Cancer Center, University of Kentucky, Lexington, KY, 40536, USA

Abstract

Dysregulated metabolism can fuel cancer by altering the production of bioenergetic building blocks and directly stimulating oncogenic gene expression programs. However, relatively few optical methods for the direct study of metabolites in cells exist. To address this need and facilitate new approaches to cancer treatment and diagnosis, here we report an optimized chemical approach to detect the oncometabolite fumarate. Our strategy employs diaryl tetrazoles as cell-permeable photoinducible precursors to nitrileimines. Uncaging these species in cells and cell extracts enables them to undergo 1,3-dipolar cycloaddition reactions with endogenous dipolarophile metabolites such as fumarate, forming pyrazoline cycloadducts that can be readily detected by their intrinsic fluorescence. The ability to photolytically uncage diaryl tetrazoles provides greatly improved sensitivity relative to previous methods, and enables the facile detection of dysregulated fumarate metabolism via biochemical activity assays, intracellular imaging, and flow cytometry. Our studies showcase a novel intersection of bioorthogonal chemistry and metabolite reactivity that can be applied for biological profiling, imaging, and diagnostic applications.

Table of Contents

Dysregulated levels of “oncometabolites” fuel cancer by directly stimulating oncogenic signaling. Here we report an optimized photoinducible 1,3-dipolar cycloaddition reaction that can be used to profile dysregulated fumarate metabolism in patient tumor samples, and demonstrate its application for the first time in imaging experiments. This novel intersection of bioorthogonal chemistry and metabolite reactivity may enable future applications in metabolite profiling, imaging, and diagnostics.

Supporting information for this article is given via a link at the end of the document.

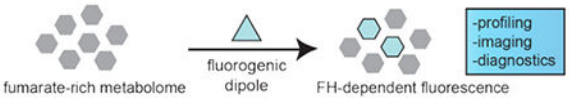

Keywords

metabolism; epigenetics; bioorthogonal; fluorescent; cycloaddition

An emerging concept in modern oncology is the direct modulation of tumorigenic signaling by cellular metabolism.[1–2] One striking example occurs in the genetic cancer predisposition syndrome hereditary leiomyomatosis and renal cell carcinoma (HLRCC).[3–5] In this disease, mutation of the TCA cycle enzyme fumarate hydratase (*FH*) causes the hyperaccumulation of fumarate,[6] an "oncometabolite" which can directly alter gene expression programs.[7–9] HLRCC tumors are highly invasive and prone to metastasis, and the current standard of care is aggressive surgical resection.[10] In addition to *FH*'s driver role in HLRCC, dysregulated levels of fumarate have been implicated in several pathophysiological contexts, including diabetes,[11] non-hereditary kidney cancer,[12–13] neuroblastoma,[14] colorectal cancer,[15–16] and tumors of the adrenal gland.[13] Methods to sensitively detect fumarate thus have the potential to provide insights into the fundamental biology of oncometabolism, as well as to facilitate new approaches to cancer treatment and diagnosis.

Fumarate can be distinguished from many cellular metabolites because it is a dipolarophile.[17] Recently, we demonstrated this property could be exploited for reactivity-based detection of cells harboring oncometabolic mutations in *FH*.[18] This method stemmed from the discovery that nitrileimine dipoles (themselves derived from hydrazonyl chloride precursors) readily react with fumarate to form highly fluorescent pyrazoline cycloadducts in aqueous solution.[18–19] Applying this reaction to profile enzymatic fumarate production allowed the differentiation of *FH* mutant and wild type cell lines derived from HLRCC patients.[18] In addition to providing a highly sensitive method to assay fumarate without mass spectrometry, this initial study established a novel application of bioorthogonal chemistry: the sensitive detection of endogenous dipolarophile-rich metabolomes produced by disease-relevant mutations (Fig. 1a).

Despite this notable progress, several challenges remain in the fluorogenic detection of fumarate. In particular, our first-generation approach suffered from limited sensitivity due to the susceptibility of hydrazonyl chlorides to undergo competing hydrolysis reactions at physiological pH (Fig. S1).[20–21] This prevented detection of endogenous fumarate, and instead required exogenous malate be added to cell extracts to amplify FH-dependent fumarate production.[18] Besides introducing additional technical processing steps this approach also requires cell lysis, and thus may offer an incomplete picture of intracellular FH activity. In contrast, an optimized method for profiling oncometabolite accumulation would be capable of detecting endogenous fumarate, with cellular or subcellular resolution. These considerations prompted us to explore 2,5-diaryl tetrazoles as an alternative class of fumarate detection reagents (Fig. 1b).[22] Diaryl tetrazoles are known to efficiently form nitrileimine dipoles upon photolysis by high energy (290 nm) UV light,[23–24] and have

previously been applied as bioorthogonal reagents for the detection of alkene-labeled proteins in live cell imaging applications.[25–27] Although more challenging to synthesize than hydrazonyl chlorides, we reasoned these molecules may hold multiple advantages for the detection of endogenous fumarate. First, the stability and rapid photolysis kinetics of diaryl tetrazoles would be expected to improve their per molecule yield of nitrileimine, thus enabling greater fumarate-dependent fluorophore formation. Second, increased reaction with fumarate may limit the consumption of nitrileimines by abundant water molecules, thereby reducing background fluorescence and increasing sensitivity. Third, the stable nature of tetrazoles may facilitate their delivery to the mitochondria,[28–29] where FH activity resides, and undergoes disruption in HLRCC.[10] This last advantage holds promise both from the perspective of increasing the selectivity of this method, by allowing fumarate to be differentiated from non-mitochondrial dipolarophiles, as well as for its potential to enable profiling of *FH* mutational status in living cells.

To explore this concept, we synthesized two novel diaryl tetrazoles and evaluated them as oncometabolite detection agents (Scheme 1). Our probe design employs a 2,5-diphenyl tetrazole core, and is based on a class of hydrazonyl chlorides our laboratory had previously demonstrated could be applied for fluorogenic fumarate profiling.[18] A key finding of those prior studies was the discovery that an electron withdrawing ethyl ester at the *para* position of the benzaldehyde-derived portion facilitated rapid reaction of nitrileimines with fumarate, as well as the formation of pyrazoline fluorophores with spectra suitable for excitation by UV- or two-photon lasers.[18, 30] Based on this precedent, as well as the literature, we reasoned replacement of the *para*-ethyl ester with a 2-azido ethyl carboxamide moiety should yield tetrazoles of similar reactivity and fluorogenicity to previously described probes, while also enabling late-stage introduction of synthetic tags for mitochondrial targeting. To synthesize parent tetrazole **1** we used a variant of the Kakehi tetrazole synthesis (Scheme 1).[31] Triphenylphosphoniums and related lipophilic cations have previously demonstrated broad utility targeting small molecules and imaging probes to the mitochondria.[29, 32] Therefore, with an eye towards cellular studies, we further conjugated this molecule to a triphenylphosphonium alkyne via Cu-catalyzed [3+2] cycloaddition to afford elaborated mitochondrial targeted tetrazole **2** (Scheme 1). These studies define an effective synthesis of multifunctional nitrileimine precursors for fumarate detection.

Tetrazole **1** possesses a single major absorbance peak at 280 nm (Fig. 2). Photoirradiation of **1** (100 μM) using a UV transilluminator (302 nm) in the presence of fumarate (10 mM) was accompanied by formation of a fluorescent pyrazoline product (λ_{ex} = 372 nm, λ_{em} = 538 nm, Fig. S1). Fluorescence required the presence of fumarate, as well as UV light (Fig. 2a-b). Next we compared tetrazole **1** with hydrazonyl chloride **3**, a previously optimized fluorescent fumarate detection reagent. Tetrazole **1** exhibited a greater fluorescence increase (395-fold versus 80-fold) as well as an improved limit of detection for fumarate (25 μM versus 100 μM) than did the previous reagent (Fig. 2c-d).[18] Reactions of fumarate with tetrazole **1** exhibited low background and, in contrast to hydrazonyl chlorides, no sign of hydrolysis products in LC-MS analysis (Fig. S1a-b). The observation that photorelease favors formation of fumarate-derived pyrazolines (signal) relative to fluorescent hydrolysis products (noise) is consistent with previous findings that nitrileimine cyclization kinetics are

rapid relative to hydrolysis.[20, 25] Furthermore, these studies imply hydrazonyl chlorides form fluorescent background products via nitrileimine-independent mechanisms which tetrazoles do not engage in, such as direct hydrolysis (Fig. S1c). A notable feature of our strategy is that it is not limited to fumarate, but can potentially be used to detect the dysregulation of other metabolic dipolarophiles, including itaconate, gluaconate, and cis-aconitate which accumulate in a variety of pathophysiological settings.[33–35] Exploring these additional metabolite dipolarophiles, we found that cis-aconitate and itaconate also formed readily observable cycloadducts upon reaction with **1** (Fig. S2) but were less detectible than fumarate (Fig. 2e). In contrast, negligible fluorescence increase was observed after photouncaging **1** in the presence of glutaconate or crotonate. Overall, these studies establish the utility and scope of functionalized diaryl tetrazoles for the photoinducible fluorescent detection of dipolarophile metabolites.

Next we aimed to assess the ability of these reagents to detect *FH* mutation in HLRCC tumor and patient samples. Our previous studies have demonstrated that hydrazonyl chloride-derived nitrileimines can be used to quantify cellular FH activity by detecting the production of fumarate from malate in cell extracts.[18] To extend this approach into more physiologically relevant models of cancer, we applied tetrazole **1** to analyze FH activity in tumor specimens derived from an HLRCC patient (*FH* −/−), healthy tissue isolated from adjacent kidney cortex (*FH*+/+) as well as HLRCC and non-HLRCC xenografts (UOK262 cells, *FH*−/−; UOK121, *FH*+/+).[36–37] Cell extracts from each sample were incubated with malate, quenched with a solution of **1** in acetonitrile, subjected to photolysis at 302 nm, and analyzed for fluorescence (Fig. 3a). A calibration curve revealed addition of malate to lysates caused production of ~50-700 μM fumarate, which falls well within the linear range of detection (Fig. S3a-b). Using this approach, we observed an 8.3-fold difference in fluorescence intensity between HLRCC and non-HLRCC xenograft samples, and a 3.5-fold decreased FH activity signal in primary HLRCC tumors relative to healthy adjacent kidney cortex (Fig. 3b). As expected, FH activity quantified by **1** was anti-correlated with tissue fumarate levels measured by GC-MS analysis (R^2 = 0.99; Fig. S3c). To further streamline this approach, we next examined whether tetrazole **1** was capable of detecting differences in endogenous metabolite dipolarophiles triggered by *FH* mutation including, but not necessarily limited to, fumarate. Using a simple one-step metabolite extraction protocol, we found that photoirradiation of **1** followed by fluorescence analysis allowed modest, but significant, differentiation of metabolomes derived from FH-deficient and replete tumors and tissue specimens (Fig. 3c). Comparison with GC-MS measurements of fumarate from patient tissues revealed a reduced dynamic range of fluorogenic detection (Fig. S3d), potentially reflecting a limitation of our method arising from incomplete reaction of **1**, or cross-reactivity with other endogenous metabolite dipolarophiles. These studies demonstrate the feasibility of using photoinducible nitrileimines to detect the endogenous metabolomic consequences of *FH* mutation in primary tumor samples.

Finally, we evaluated tetrazole probes **1**-**2** for their ability to detect changes in fumarate concentrations in living cells (Fig. 4). As an initial proof-of-concept, we evaluated untargeted probe **1** for its ability to detect cells treated with dimethyl fumarate (DMF; trade name Tecfidera), a multiple sclerosis drug that has a similar, albeit more reactive,

dipolarophile core as the HLRCC oncometabolite.[38] Cells were treated simultaneously with DMF (100 μM) or vehicle, and tetrazole **1** (100 μM) for 2 h . Treated and untreated cells were then washed, photoirradiated at 302 nm for 2 min, and imaged immediately. Trypan blue indicated that cells remain viable following nitrilimine photouncaging (Fig. S4); however, care was taken to perform imaging experiments immediately due to the known phototoxicity of 302 nm light. Confocal microscopy analysis revealed clear fluorescence in the green channel corresponding to the DMF-derived product of **1** (λ_{ex} = 820 nm two-photon, em = 525/20 nm; Fig. 4a-j, Fig. S5). Unexpectedly, despite possessing well-characterized cytosolic and nuclear targets,[39] a large portion of DMF-dependent fluorescence co-localized with the mitochondria (Fig. 4a-j)(. This suggests probe **1** itself may preferentially localize to or react in this organelle. In addition to enabling us to optimize our protocol for detection of the fumarate chemotype, these studies suggest diaryl tetrazoles may have utility in studying the cellular occupancy of small molecule drugs which harbor dipolarophiles embedded in their structure.[39]

To build on these studies, we next tested mitochondrial tetrazole **2** for its ability to detect FH-dependent changes in metabolic dipolarophiles in living cells (Fig. 4k-v, Fig. S6). This experiment applies mitochondrial probe **2** to compare patient-derived immortalized HLRCC cells (UOK262 and UOK268) to isogenic rescue cell lines, in which wild-type FH has been reintroduced by lentiviral transduction (UOK262WT and UOK268WT).[36–37] As above, cell lines were pre-loaded with **2** (100 μM, 2 h), photoirradiated, and imaged immediately. Confocal microscopy analysis revealed overlapping fluorescence in the green channel corresponding to the fumarate-derived product of **2** (λ_{ex} = 820 nm two-photon, em = 525/20 nm) which clearly co-localized with MitoTracker Green, confirming mitochondrial targeting. Using quantitative confocal microscopy to more accurately compare *FH*−/− and *FH*+/+ HLRCC cells led to the observation of modest, but significantly increased, fluorescence in the FH-deficient lines (Fig. 4u). Quantification of this effect over a larger population of cells using flow cytometry indicated an ~1.5-fold increase in fluorescence in *FH*−/− versus wild type HLRCC cells (Fig. 4v), consistent with our solution-based measurements above. Untargeted probe **1** also detected increased dipolarophile load in *FH*−/− cells, albeit with a slightly more limited range, and exhibited mitochondrial localization similar to the DMF studies (Fig. S7). Overall, these data indicate that diaryl tetrazoles possess the requisite sensitivity to detect fluctuations in endogenous mitochondrial dipolarophiles triggered by *FH* mutation in living cells.

In conclusion, here we have reported a photoinducible fluorogenic probe for the oncometabolite fumarate. Our studies define HLRCC as a novel cancer context in which the normally bioorthogonal nitrileimine-alkene cycloaddition can be exploited to detect changes in endogenous metabolism triggered by *FH* mutation. Furthermore, we demonstrate for the first time that this reaction can be applied to directly detect *FH* mutation in patient-derived tumor samples and also to image *FH* mutational status in living cells. An important conceptual aspect of our strategy that is distinct from traditional small molecule fluorogenic sensors is that it can detect a variety of metabolite dipolarophiles (Fig. 2e). This means it is most appropriately applied for the detection of large changes in fumarate, as occur in HLRCC. It also raises the possibility of applying this method to study other physiological

contexts characterized by dipolarophile hyperaccumulation such as macrophage activation (itaconate), mitochondrial disorders (cis-aconitate), and tyrosinemia (fumarylacetoacetate).[33–35] Validating these applications will benefit from further analyses of the metabolome-wide reactivity of nitrileimines, which help better define the scope of dipolarophiles that may be studied using this method, as well as non-specific background.[40] While our studies validate the use of diaryl tetrazoles to detect *FH*-deficient tumors, one limitation is the relatively small dynamic range they afford for endogenous fumarate detection. We envision this may be addressed in the future by developing approaches to co-deliver FH substrates to the mitochondria (in order to facilitate signal amplified turnover as in our enzyme profiling studies) as well as by exploring alternative detection strategies, for example using the nitrileimine-fumarate cycloaddition to trap radiotracers or fluorophores that are otherwise freely permeable in HLRCC cells.[41] This strategy will also benefit from the use of two-photon excitable tetrazoles,[30] which may limit phototoxicity and enable imaging over extended time frames. Finally, it is important to note that many examples have shown that hereditary cancer syndromes often highlight broadly active mechanisms of tumorigenesis.[42–43] Therefore, in addition to pathology and imaging, methods to sensitively detect FH activity are of utmost interest as basic research tools to identify new biological contexts where fumarate plays a pathophysiological role. In the future, these methods may facilitate high-throughput analyses of how levels of this oncometabolite are impacted by diverse genetic, biological, and small molecule stimuli. Overall, our studies illuminate a distinct aspect of cancer metabolism that can be interrogated using bioorthogonal chemistry, and set the stage for new applications of this reactivity in biology, imaging and diagnostic methods.

Supplementary Material

Refer to Web version on PubMed Central for supplementary material.

Acknowledgements

We thank Dr. Martin Schnermann (NCI) for helpful discussions. This work was supported by the Intramural Research Program of the NIH, National Cancer Institute (ZIA BC011488-02).

References

[1]. Kinnaird A, Zhao S, Wellen KE, Michelakis ED, Nat Rev Cancer 2016, 16, 694–707. [PubMed: 27634449]

[2]. Meier JL, ACS Chem Biol 2013, 8, 2607–2621. [PubMed: 24228614]

[3]. Launonen V, Vierimaa O, Kiuru M, Isola J, Roth S, Pukkala E, Sistonen P, Herva R, Aaltonen LA, Proc Natl Acad Sci U S A 2001, 98, 3387–3392. [PubMed: 11248088]

[4]. Tomlinson IP, Alam NA, Rowan AJ, Barclay E, Jaeger EE, Kelsell D, Leigh I, Gorman P, Lamlum H, Rahman S, et al., Nat Genet 2002, 30, 406–410. [PubMed: 11865300]

[5]. Zengeya TT, Kulkarni RA, Meier JL, Org Lett 2015, 17, 2326–2329. [PubMed: 25915096]

[6]. Pollard PJ, Briere JJ, Alam NA, Barwell J, Barclay E, Wortham NC, Hunt T, Mitchell M, Olpin S, Moat SJ, et al., Hum Mol Genet 2005, 14, 2231–2239. [PubMed: 15987702]

[7]. Sudarshan S, Sourbier C, Kong HS, Block K, Valera Romero VA, Yang Y, Galindo C, Mollapour M, Scroggins B, Goode N, et al., Mol Cell Biol 2009, 29, 4080–4090. [PubMed: 19470762]

[8]. Kinch L, Grishin NV, Brugarolas J, Cancer Cell 2011, 20, 418–420. [PubMed: 22014567]

[9]. Sciacovelli M, Goncalves E, Johnson TI, Zecchini VR, da Costa AS, Gaude E, Drubbel AV, Theobald SJ, Abbo SR, Tran MG, et al., Nature 2016, 537, 544–547. [PubMed: 27580029]

[10]. Grubb RL, Franks ME, Toro JR, Hurley K, Glenn GM, Choyke P, Coleman J, Torres-Cabala C, Merino MJ, Zbar B, et al., J Urology 2005, 173, 379–379.

[11]. Alderson NL, Wang Y, Blatnik M, Frizzell N, Walla MD, Lyons TJ, Alt N, Carson JA, Nagai R, Thorpe SR, et al., Arch Biochem Biophys 2006, 450, 1–8. [PubMed: 16624247]

[12]. N. Cancer Genome Atlas Research, Linehan WM, Spellman PT, Ricketts CJ, Creighton CJ, Fei SS, Davis C, Wheeler DA, Murray BA, Schmidt L, et al., N Engl J Med 2016, 374, 135–145. [PubMed: 26536169]

[13]. Lehtonen HJ, Kiuru M, Ylisaukko-Oja SK, Salovaara R, Herva R, Koivisto PA, Vierimaa O, Aittomaki K, Pukkala E, Launonen V, et al., J Med Genet 2006, 43, 523–526. [PubMed: 16155190]

[14]. Fieuw A, Kumps C, Schramm A, Pattyn F, Menten B, Antonacci F, Sudmant P, Schulte JH, Van Roy N, Vergult S, et al., Int J Cancer 2012, 130, 2599–2606. [PubMed: 21796619]

[15]. Bateman LA, Ku WM, Heslin MJ, Contreras CM, Skibola CF, Nomura DK, ACS Chem Biol 2017, 12, 905–911. [PubMed: 28229591]

[16]. Ashrafian H, O'Flaherty L, Adam J, Steeples V, Chung YL, East P, Vanharanta S, Lehtonen H, Nye E, Hatipoglu E, et al., Cancer Res 2010, 70, 9153–9165. [PubMed: 20978192]

[17]. Jewett JC, Bertozzi CR, Chem Soc Rev 2010, 39, 1272–1279. [PubMed: 20349533]

[18]. Zengeya TT, Garlick JM, Kulkarni RA, Miley M, Roberts AM, Yang Y, Crooks DR, Sourbier C, Linehan WM, Meier JL, J Am Chem Soc 2016, 138, 15813–15816. [PubMed: 27960310]

[19]. An P, Yu Z, Lin Q, Chem Commun (Camb) 2013, 49, 9920–9922. [PubMed: 24036983]

[20]. Wang XS, Lee YJ, Liu WR, Chem Commun (Camb) 2014, 50, 3176–3179. [PubMed: 24519550]

[21]. Zheng SL, Wang Y, Yu Z, Lin Q, Coppens P, J Am Chem Soc 2009, 131, 18036–18037. [PubMed: 19928921]

[22]. Lim RK, Lin Q, Acc Chem Res 2011, 44, 828–839. [PubMed: 21609129]

[23]. Clovis JS, Eckell A, Huisgen R, Sustmann R, Chemische Berichte 1967, 100, 60–70.

[24]. Wang Y, Vera CI, Lin Q, Org Lett 2007, 9, 4155–4158. [PubMed: 17867694]

[25]. Wang Y, Song W, Hu WJ, Lin Q, Angew Chem Int Ed Engl 2009, 48, 5330–5333. [PubMed: 19544336]

[26]. Song W, Wang Y, Qu J, Lin Q, J Am Chem Soc 2008, 130, 9654–9655. [PubMed: 18593155]

[27]. Song W, Wang Y, Qu J, Madden MM, Lin Q, Angew Chem Int Ed Engl 2008, 47, 2832–2835. [PubMed: 18311742]

[28]. Dickinson BC, Srikun D, Chang CJ, Curr Opin Chem Biol 2010, 14, 50–56. [PubMed: 19910238]

[29]. Dickinson BC, Chang CJ, J Am Chem Soc 2008, 130, 9638–9639. [PubMed: 18605728]

[30]. Yu Z, Ohulchanskyy TY, An P, Prasad PN, Lin Q, J Am Chem Soc 2013, 135, 16766–16769. [PubMed: 24168622]

[31]. Ito S, Tanaka Y, Kakehi A, Kondo K, Bulletin of the Chemical Society of Japan 1976, 49, 1920–1923.

[32]. Murphy MP, Smith RA, Annu Rev Pharmacol Toxicol 2007, 47, 629–656. [PubMed: 17014364]

[33]. Gerstner B, Gratopp A, Marcinkowski M, Sifringer M, Obladen M, Buhrer C, Pediatr Res 2005, 57, 771–776. [PubMed: 15774829]

[34]. Crooks DR, Maio N, Lane AN, Jarnik M, Higashi RM, Haller RG, Yang Y, Fan TW, Linehan WM, Rouault TA, J Biol Chem 2018, 293, 8297–8311. [PubMed: 29523684]

[35]. Cordes T, Wallace M, Michelucci A, Divakaruni AS, Sapcariu SC, Sousa C, Koseki H, Cabrales P, Murphy AN, Hiller K, et al., J Biol Chem 2016, 291, 14274–14284. [PubMed: 27189937]

[36]. Yang Y, Valera V, Sourbier C, Vocke CD, Wei M, Pike L, Huang Y, Merino MA, Bratslavsky G, Wu M, et al., Cancer Genet 2012, 205, 377–390. [PubMed: 22867999]

[37]. Yang Y, Valera VA, Padilla-Nash HM, Sourbier C, Vocke CD, Vira MA, Abu-Asab MS, Bratslavsky G, Tsokos M, Merino MJ, et al., Cancer Genet Cytogenet 2010, 196, 45–55. [PubMed: 19963135]

[38]. Linker RA, Gold R, Curr Neurol Neurosci Rep 2013, 13, 394. [PubMed: 24061646]

[39]. Blewett MM, Xie J, Zaro BW, Backus KM, Altman A, Teijaro JR, Cravatt BF, Sci Signal 2016, 9, rs10. [PubMed: 27625306]

[40]. Li Z, Qian L, Li L, Bernhammer JC, Huynh HV, Lee JS, Yao SQ, Angew Chem Int Ed Engl 2016, 55, 2002–2006. [PubMed: 26640085]

[41]. Carroll L, Evans HL, Aboagye EO, Spivey AC, Org Biomol Chem 2013, 11, 5772–5781. [PubMed: 23907155]

[42]. Erez A, DeBerardinis RJ, Nat Rev Cancer 2015, 15, 440–448. [PubMed: 26084394]

[43]. Herman JG, Latif F, Weng Y, Lerman MI, Zbar B, Liu S, Samid D, Duan DS, Gnarra JR, Linehan WM, et al., Proc Natl Acad Sci U S A 1994, 91, 9700–9704. [PubMed: 7937876]

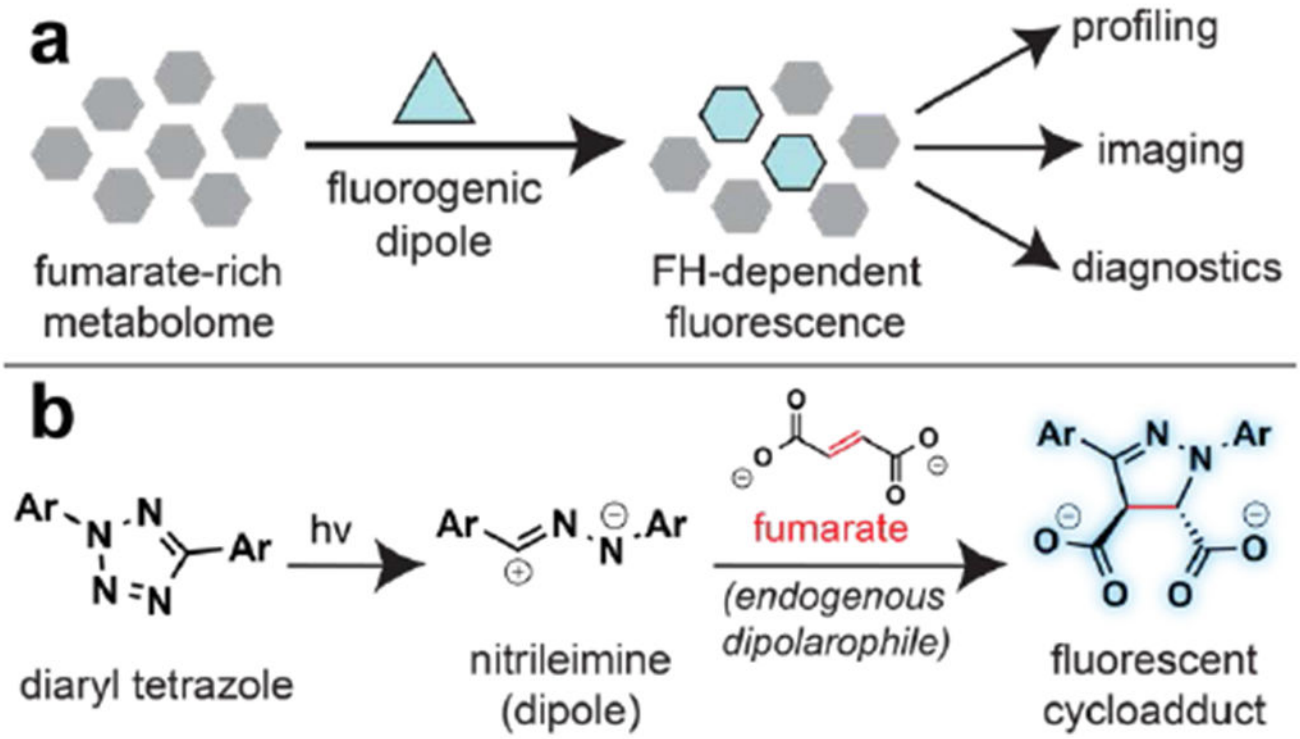

Figure 1.

Photoinducible detection of the oncometabolite fumarate. (a) General schematic for bioorthogonal detection of fumarate-rich metabolomes using fluorogenic dipoles. (b) Diaryl tetrazoles are photoinducible precursors that form nitrileimines which undergo fluorogenic reactions with fumarate.

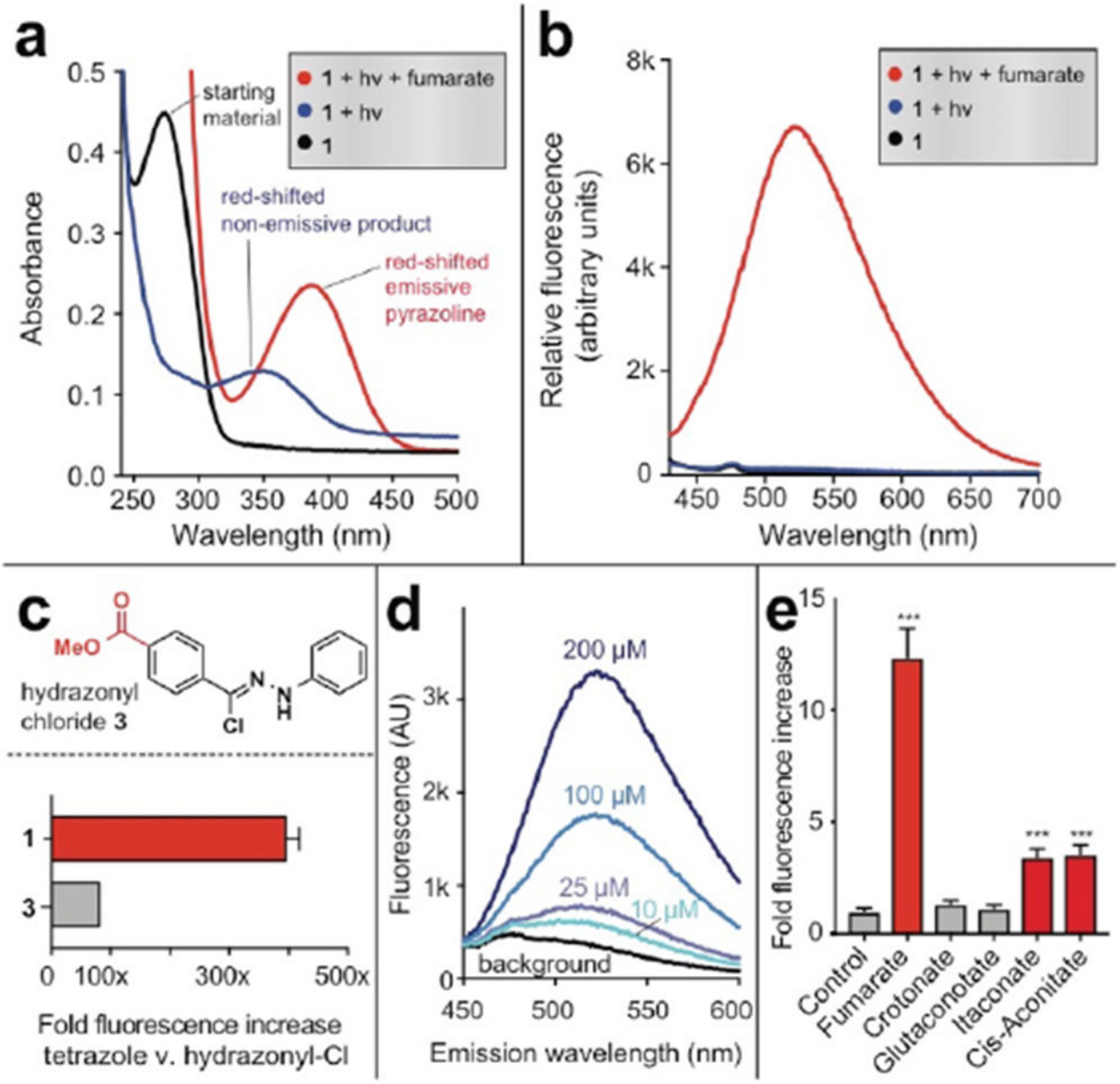

Figure 2.

Fluorogenic detection of fumarate by tetrazole **1**. (a) Absorbance spectra of tetrazole **1** following photolysis in the presence or absence of 10 mM fumarate. (b) Fluorescence spectra (λ_{ex} = 410 nm) of tetrazole **1** following photolysis in the presence or absence of 10 mM fumarate. Reaction conditions: 100 µM tetrazole **1**, 10 mM fumarate, 5% DMSO in PBS (pH 7.2), hν= 302 nm, 2 min. (c) Comparison of fluorescent detection of fumarate (10 mM) by tetrazole **1** (100 µM, hν=302 nm, 2 min) and previously described hydrazonyl chloride **3** (**1** (100 µM, 1 h). (d) Limit of detection of fumarate by tetrazole **1**. Data is representative of 3 replicates. (e) Fluorescent detection of other metabolite dipolarophiles by tetrazole **1** (λ_{ex} = 410 nm, λ_{em} = 540 nm) Reaction conditions: 100 µM tetrazole **1**, 200 µM

metabolite, sodium phosphate buffer pH 7.0 (1:1), hν= 302 nm, 2 min. Statistical significance was determined by unpaired *t* test ($n = 3$, ***$P < 0.001$).

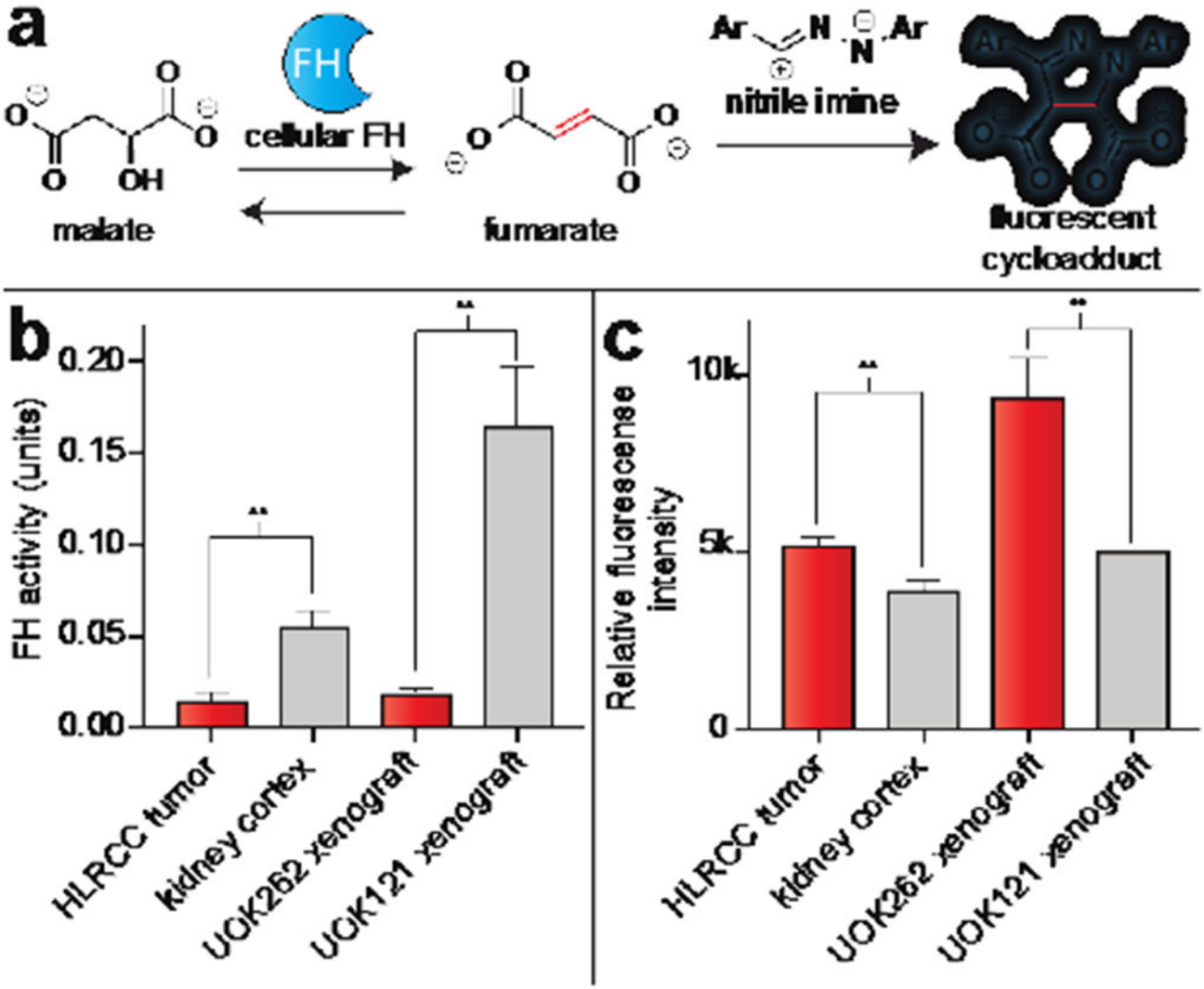

Figure 3.

Detection of FH activity and endogenous dipolarophiles from tumor specimens using tetrazole **1**. Analysis was performed from 3 different HLRCC tumors and kidney cortex samples from same patient, and 3 separate xenografts from 3 separate mice. (a) Schematic for signal-amplified FH activity assay. (b) Detection of differences in endogenous FH activity in tumor samples by tetrazole **1**. Tumor lysates were first incubated with *L*-malic acid (25 mM, 1 h), then treated with tetrazole **1** (150 μM), photoirradiated (302 nm, 2 min), and analyzed by fluorimetry (λ_{ex} = 380 nm, λ_{em} = 540 nm). Lower fluorescence corresponds to lower FH activity, as expected upon *FH* mutation. (c) Differences in endogenous dipolarophile levels in tumor samples by tetrazole **1**. Endogenous metabolites extracted from tumors were treated with tetrazole **1** (250 μM), photoirradiated (302 nm, 2 min) and analyzed by fluorimetry (λ_{ex} = 410 nm, λ_{em} = 540 nm). Higher fluorescence corresponds to higher endogenous dipolarophile concentrations, as expected upon *FH* mutation. Statistical significance was analysed by unpaired *t* test ($n = 3$, $^{**}P < 0.01$).

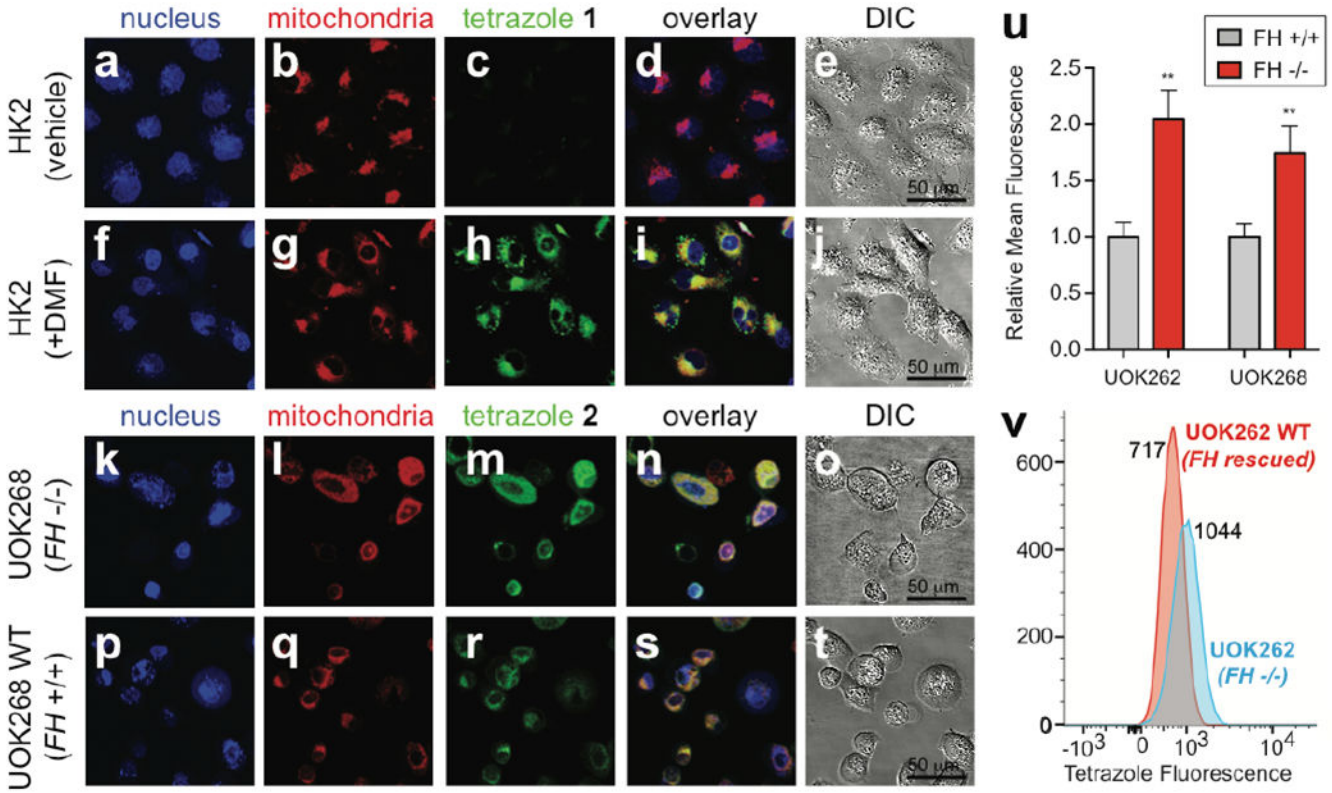

Figure 4.

Detection of dipolarophiles in living cells using tetrazoles. (a-t) Images from confocal microscopy experiments. HK2 cells were simultaneously treated with tetrazole **1** (100 μM, 2 h) and vehicle (DMSO, 2 h, a-e) or dimethylfumarate (DMF) (100 μM, 2 h, f-j). UOK268 (k-o) and UOK268WT (p-t) cells were treated with tetrazole **2** (100 μM, 2 h). All cells (a-t) were treated with MitoTracker Green FM (100 nM, 30 min) and DRAQ5 (200 nM, 30 min), washed, and, photoirradiated (302 nm, 2 min). Confocal images displayed are obtained for DRAQ5 (633 nm HeNe633 laser, false-colored blue, a,f,k,p), MitoTracker Green (488 nm argon laser, false-colored red, b,g,l,q), and tetrazole (820 nm two-photon laser, green, c,h,m,r). (d,i,n,s) represents overlay of confocal images and (e,j,o,t) represents differential interference contrast (DIC) microscopy images with a 50 μm scale bar. (u) Mean fluorescence intensities of tetrazole fluorescence quantified from confocal images for UOK262 (*FH* −/−) relative to UOK262WT (*FH* +/+), and UOK268 (*FH* −/−) relative to UOK268WT (*FH* +/+). Total 10 cells were analyzed per cell line. Error bars denote SEM. Statistical significance analysed by unpaired *t* test ($n = 3$, ***$P < 0.001$). (v) Histograms obtained via flow cytometry analysis of UOK262 (*FH* −/−) and UOK262WT (*FH* +/+) cells treated with tetrazole **2** (100 μM, 2 h; followed by washing and photoirradiation).

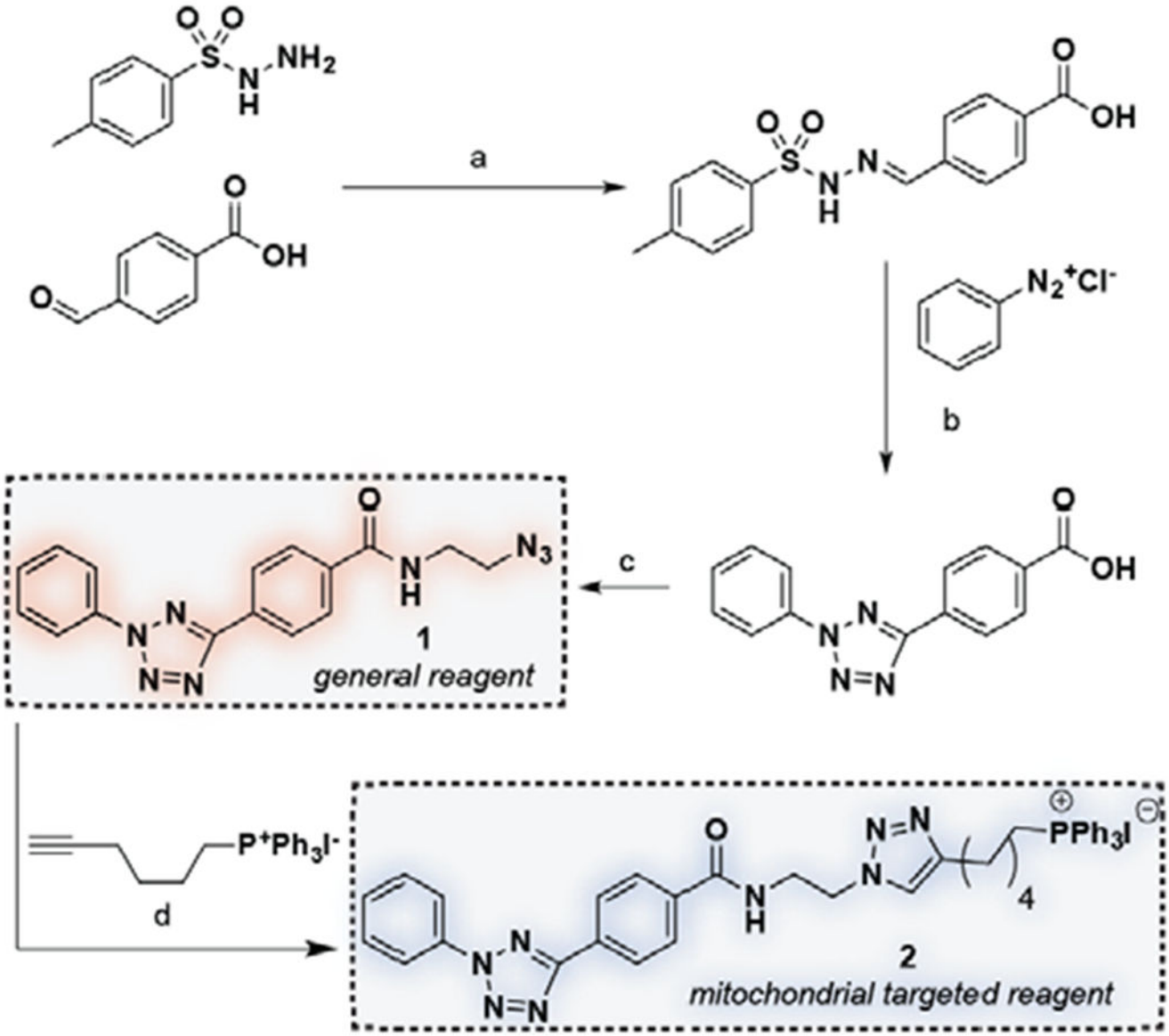

Scheme 1.

Synthesis of diaryl tetrazoles used in this study. (a) EtOH, reflux, 4 h, 95%. (b) Pyridine, 0 °C to rt, 24 h, 63%. (c) 2-azidoethylene diamine, HBTU, NMM, DMF, rt, 2 h, 91%. (d) CuI, DCM, reflux, 72h, 45%.